Project No. 037005

CECILIA

Central and Eastern Europe Climate Change Impact and Vulnerability Assessment

Specific targeted research project

1.1.6.3.I.3.2: Climate change impacts in central-eastern Europe

D7.3: Key species concentrations files from higher resolution runs (10x10 km) for control run and future projection

Due date of deliverable: 1st March 2009
Actual submission date: 1th July 2009

Start date of project: 1st June 2006 Duration: 43 months

Lead contractor for this deliverable: CUNI

Project co-funded by the European Commission within the Sixth Framework Programme (2002-2006)		
Dissemination Level		
PU	Public	X
PP	Restricted to other programme participants (including the Commission Services)	
RE	Restricted to a group specified by the consortium (including the Commission Services)	
CO	Confidential, only for members of the consortium (including the Commission Services)	

D7.3 – Key species concentrations files from higher resolution runs (10x10 km) for control run and future projection

CUNI

1 High resolution modelling and air quality

In many applications, particularly related to the assessment of climate-change impacts, the information on surface climate change at regional to local scale is fundamental and that is Global Circulation Models (GCMs) can hardly reproduce reasonably well. Thus, dynamical downscaling, i.e., nesting of a fine scale limited area model (or Regional Climate Model, RCM) within the GCM is the most convenient tool taking into account processes critically affected by topography and land use at high resolution in this kind of studies and especially when aiming the interactions of climate and air-quality issues. In the region of Central and Eastern Europe (CEE) the need for high resolution studies is particularly important, that is why 10 km resolution has been introduced in the EC FP6 project CECILIA. One of the main aims of the project dealing with climate change impacts and vulnerability assessment in targeted areas of CEE is the application of regional climate modelling studies at a resolution of 10 km for local impact studies in key sectors of the region.

The concentration of air pollutants depends on both anthropogenic and climate factors. However, in this study the anthropogenic emission are kept for all the time slices at the values of year 2000 to study climate effects. Longer range transport to the target regions is taken into account from simulation for the whole Europe using RCM with the resolution of 50x50 km. These simulations are used to constrain nested higher resolution runs (10x10 km) focusing in CEE both for present and future climate. The key species are ozone, sulphur, nitrogen and PM, which have a central role in tropospheric chemistry as well as the strong health impacts.

It is now well established that climatically important (radiatively active) gases and aerosols can have substantial climatic impact trough their direct and indirect effects on radiation, especially on regional scales (Qian and Giorgi, 2000, Qian et al., 2001, Giorgi et al., 2002). To study these effects requires coupling of regional climate models with atmospheric chemistry/aerosols to assess the climate forcing to the chemical composition of the atmosphere and its feedback to the radiation, eventually other components of the climate system. In this study climate is calculated using model RegCM while chemistry is solved by model CAMx. The model RegCM was originally developed and further improved by Giorgi et al. (1999) or later see e.g. in Pal et al. (2007). For more details on the use of the model see Elguindi at al. (2006).

CAMx is an Eulerian photochemical dispersion model developed by ENVIRON Int. Corp. (Environ, 2006). In version 4.40 CAMx is used for air quality modeling here, with CB-IV gas phase chemistry mechanism option, wet deposition of gases and particles. It uses mass conservative and consistent transport numerics in parallel processing. It allows for integrated "one-atmosphere" assessments of gaseous and particulate air pollution (ozone, PM2.5, PM10, air toxics) over many scales ranging from sub-urban to continental. CAMx simulates the emission, dispersion, chemical reactions and removal of pollutants in the troposphere by solving the pollutant (eulerian) continuity equation for each chemical species on a system of nested three-dimensional grids. These processes are strongly dependent on the meteorological conditions, therefore CAMx requires meteorological input from a NWP model or RCM for successful run.

2 Settings and results

Meteorological fields generated by RegCM drive CAMx transport and dry/wet deposition. Briefly, a preprocessor utility was developed which takes RegCM's outputs and convert them to fields and formats accepted by CAMx. There are problems with the anthropogenic emission inventories available, at this stage emissions from EMEP 50 x 50 km database are interpolated. Biogenic emissions of isopren and monoterpenes are calculated as a function of 2m temperature, global radiation and land-use by Guenther et al. (1993,1994). We use 23 vertical σ-levels reaching up to 70hPa at 10km of resolution for RegCM configuration, the same horizontal grid for CAMx. Initial and boundary conditions are taken from 50 km resolution run for whole Europe by Krueger et al. (2008) or Katragkou et al. (2009). In our setting CB-IV chemistry mechanism is used (Gery et al.,1989). As the first step, the distribution of pollutants is simulated off-line for four time slices of 10 years in the model couple. Period of 1991-2000 driven by reanalysis ERA40 is used for validation whereas control run 1991-2000 driven by global model ECHAM5 is used for comparison and estimate of systematic error imposed by GCM, future time slices 2041-50 and 2091-2100 provide the information on climate change impact on future air quality.

Extended validation analysis was performed for ERA 40 driven run and examples are presented here in Figs. 1 and 2.

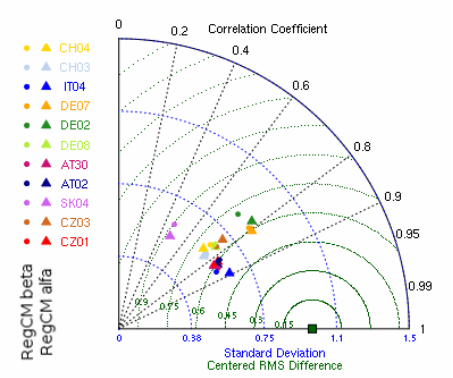

Figure 1. *Monthly average of ozone concentration, Taylor diagram of two versions of RegCM (alfa and beta–high resolution precipitation bug corrected) against observations, 1991-2000, ERA40 driven.*

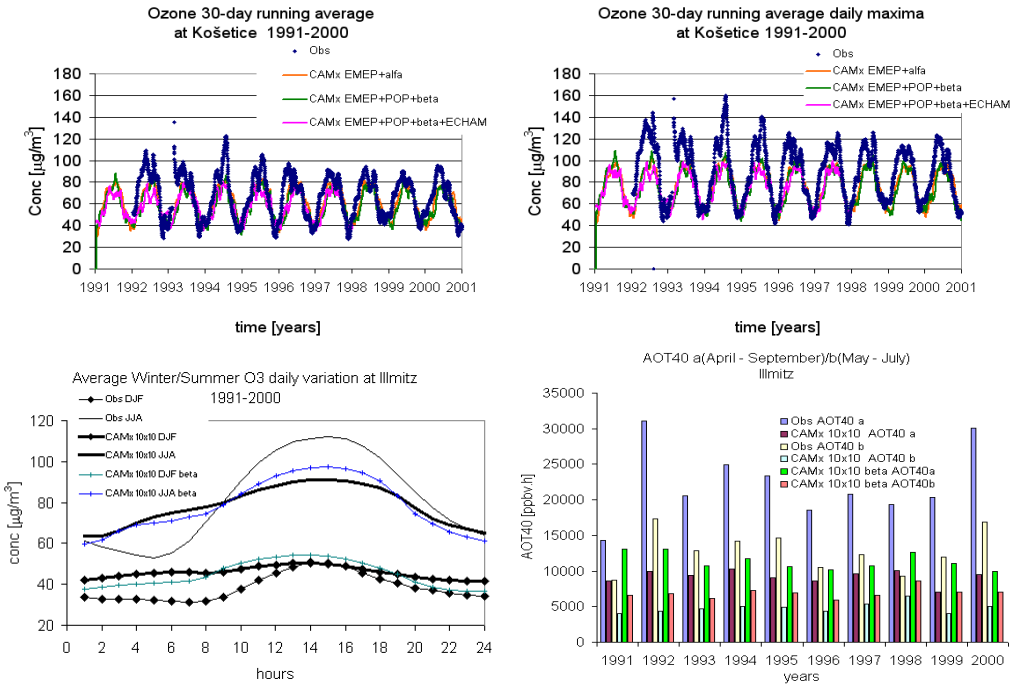

Figure 2. *Ozone characteristics from different model versions compared to observation at station Kosetice (above) and Illmitz (bottom) for 1991-2000.*

The comparison of monthly average ozone concentration is presented in Fig. 1 in terms of Taylor diagram with sensitivity test to precipitation bug. Reasonable agreement can be seen, but deeper insight into the behaviour of the outputs can be seen from time series of the ozone concentration presented in Fig. 2. Clearly, even the version with corrected high resolution precipitation bug (RegCM-beta) is underestimating daily variations, and reliability of reproducing some other parameters like AOT40 is not so high. Underestimation of the ozone concentration by the model especially during warm season appears for most stations of the Central Europe. However, high resolution runs brings slight improvement of the results for most of selected stations. Problems with emission data resolution could probably account for these deviations at least partially.

Concerning the future scenario runs, A1B results of 10 km resolution simulations for 2041-2050 and 2091-2100 time slices are presented in Fig. 3 in terms of ozone concentration difference against the control run 1991-2000 for summer season. The development of the impact on air quality can be seen not only in term of the concentration changes but e.g. in terms of number of days with exceedance of certain threshold shown in Fig. 4. Clearly, 2041-2050 time slice shows not so well developed effects for near future while at the end of century the 2091-2100 time slice indicates quite significant impact. Results for other species from the model are available as well, e.g. for exceedances of SO_2 and PM_{10} limit values, see Figs. 5 and 6. Climate change impact on other characteristics can be analysed, like AOT40 (see Fig. 7) or maximum concentrations (see Fig. 8).

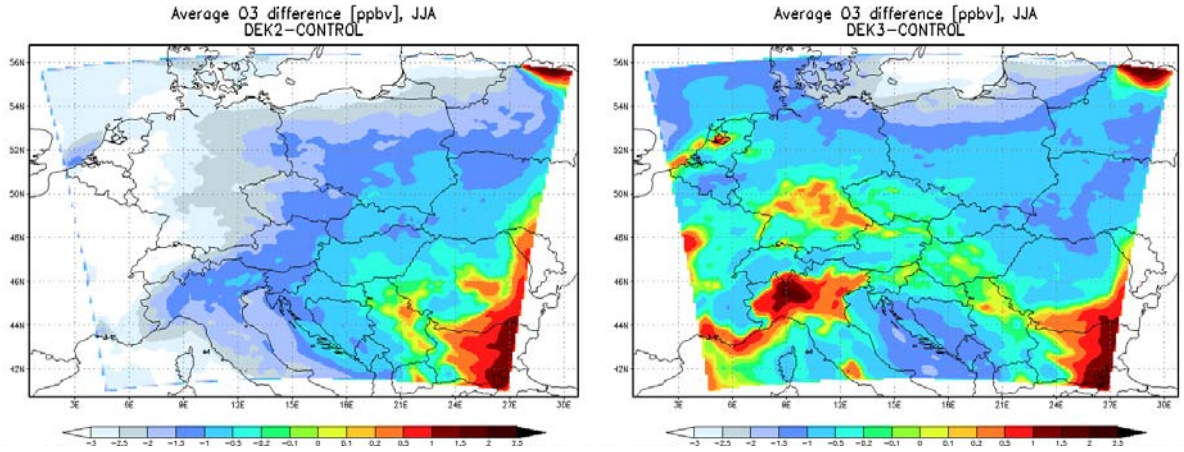

Figure 3. *Climate change impact on summer season ozone concentration (in ppbv) in terms of the difference for 2041-2050 period (left panel) and 2091-2100 period (right panel) against the control period 1991-2000.*

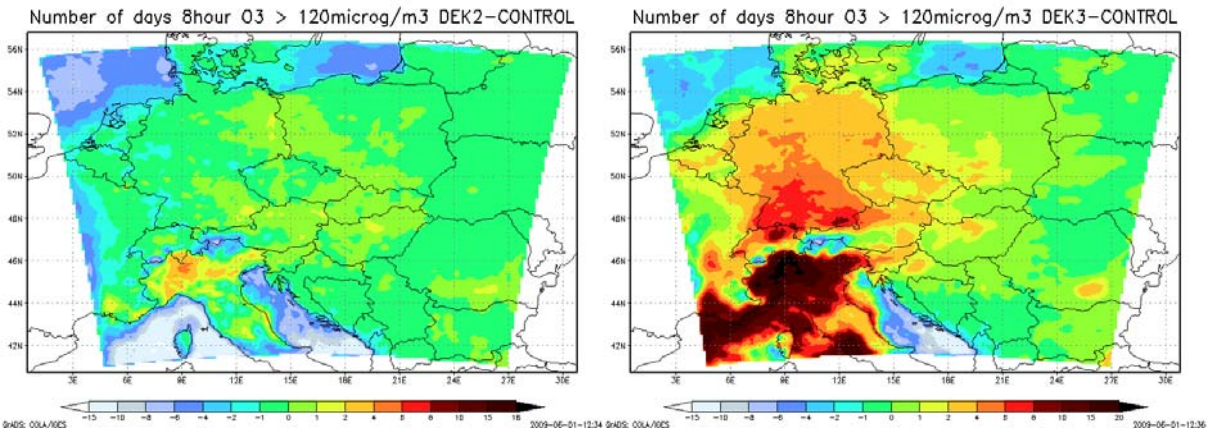

Figure 4. *Climate change impact on number of days per year with 8-hours ozone concentration above the threshold of 120 μg/m^3 in terms of the difference for 2041-2050 period (left panel) and 2091-2100 period (right panel) against the control period 1991-2000.*

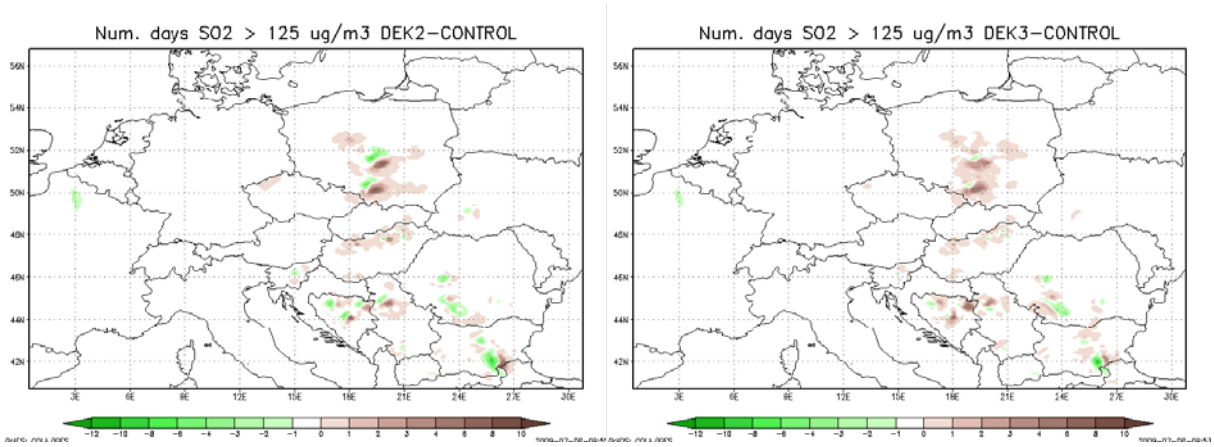

Figure 5. *Climate change impact on number of days per year with 24-hours SO_2 concentration above the threshold of 125 μg/m^3 in terms of the difference for 2041-2050 period (left panel) and 2091-2100 period (right panel) against the control period 1991-2000.*

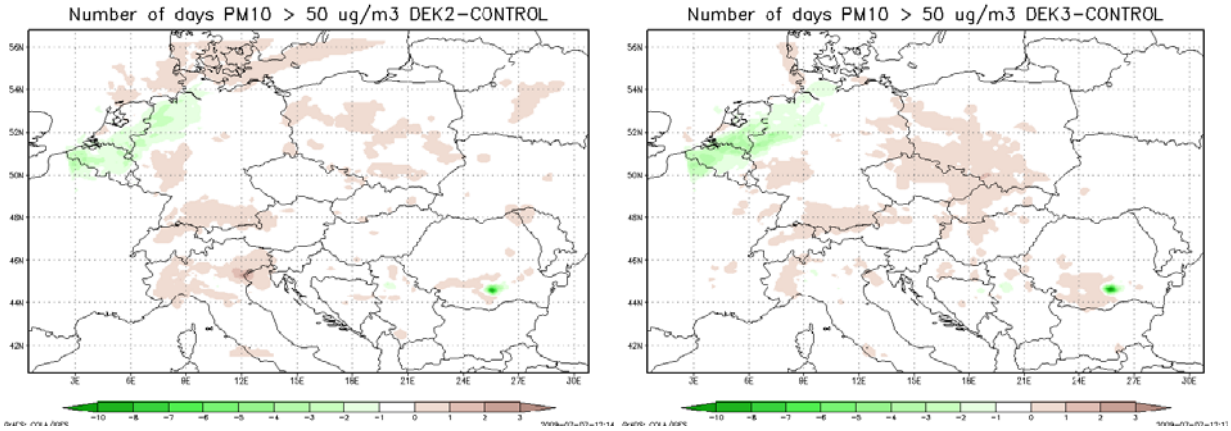

Figure 6. *Climate change impact on number of days per year with 24-hours PM_{10} concentration above the threshold of 50 μg/m^3 in terms of the difference for 2041-2050 period (left panel) and 2091-2100 period (right panel) against the control period 1991-2000.*

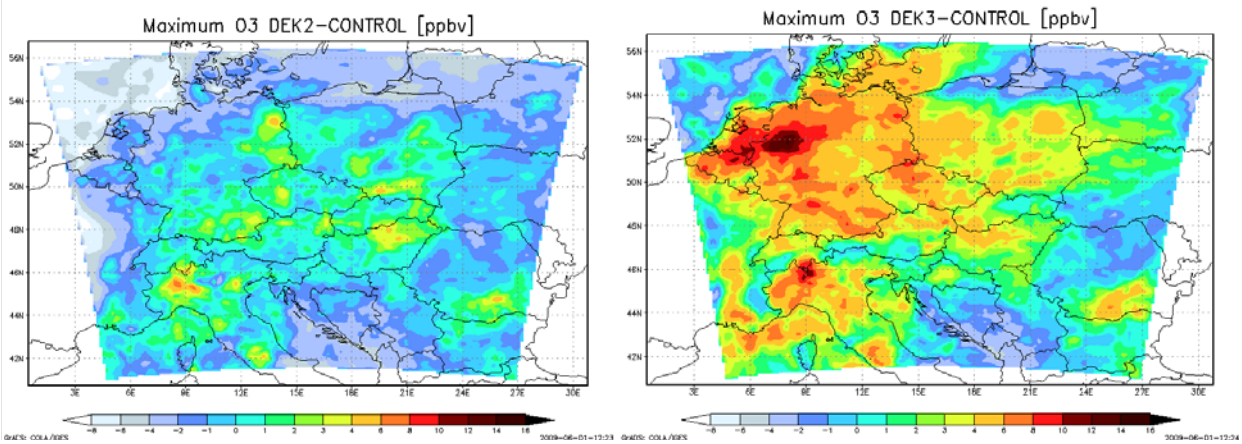

Figure 7. *Difference in average annual ozone maxima between years 2041-2050 (left panel) and 2091-2100 (right panel) against control period 1991-2000.*

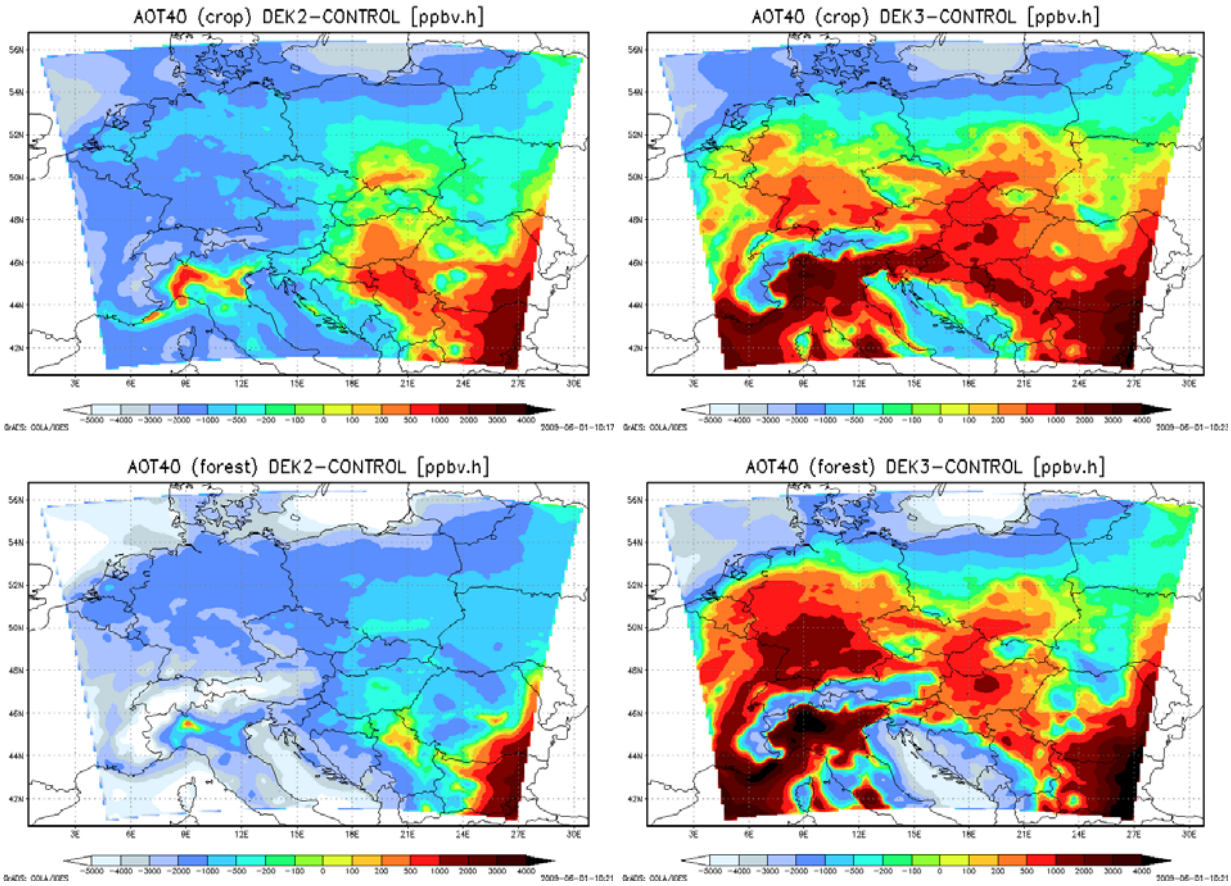

***Figure 8**. Difference in AOT40 for crop impacts assessment (May-July, upper panels) and for forest impacts assessment (April-September, lower panels) between years 2041-2050 (left panels) and 2091-2100 (right panels) against control period 1991-2000.*

BOKU

In addition to previous 50km full Europe simulations, at BOKU photochemical model runs with CAMx were performed with a spatial resolution of 10 km using the meteorological fields of RegCM3(Beta) performed at ELU for Panonia region. The configuration of CAMx was the same as for the 50 km-runs (Deliverable 7.2). The model had 12 vertical layers of varying thickness, extending up to 450 hPa. With a domain size of 118 by 98 cells, it covered Hungary, Slovakia, and Czech Republic as well as eastern Austria, southern Poland and western Romania within the area of interest of CECILIA.

As concentrations at the lateral boundaries hourly concentrations from the corresponding runs with the 50 km model were taken. Clean-air conditions were assumed at the model top. As in other runs of the project, the emissions for the year 2000 based on EMEP data with a spatial resolution of 50 km were taken for all calculated years in order to restrict differences between the decades to climate effects. For the countries Czech Republic, Austria, Slovakia, and Hungary, these emissions were distributed to a spatial resolution of 5 km.

High resolution calculations were made for three decades, namely 1991-2000 with RegCM-data driven by reanalysis ERA40 for the validation of the model, 1991-2000 with meteorological data driven by the GCM ECHAM as the control run, and for the end-century decade 2091-2100, also GCM-driven to investigate the climate response. The mid-century-decade 2041-2050 has only been calculated with 50 km resolution. Since differences in the results for ozone were small here, the calculation of this decade with 10 km resolution was skipped.

Fig. 9 shows the decadal average of the ozone volume mixing ratio for the summer season (JJA) for the control run in 10km resolution as well as the difference of this value calculated for the end-century

decade. By the end of the century the seasonal ozone volume mixing ratio average increases in the whole model domain with a gradient of the difference ranging from about 5 ppb in the west to about 1 ppb in the east. This result agrees qualitatively and quantitatively with those found in the 50 km-resolution runs (Deliverable 7.2). Differences between the runs with high and low spatial resolution were investigated in Deliverable 7.4.

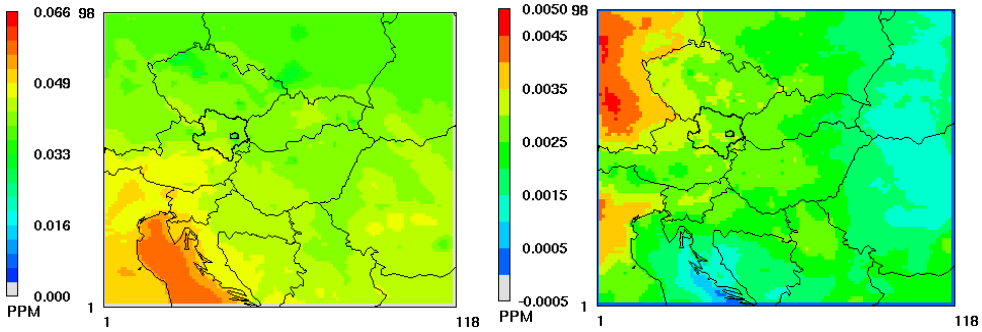

Figure 9. *Left: Decadal average (1991-2000) of the ozone volume mixing ratio in the summer season (JJA) from the control run in 10km resolution. Right: Difference in the ozone volume mixing ratio between the end-century run (2091-2100) and the control run.*

Fig. 10 displays the $AOT40_c$ values for the present day and the end-century decades calculated for BOKU domain in high 10 km resolution. The values are generally higher than in the coarse resolution run. With present day conditions (1991-2000) only over Poland and Ukraine the limit of 9 000 ppb h is not exceeded. The highest values are found over the Adriatic Sea and over Italy. With far future climate (2091-2100) a further increase is observed. The high increase over Southern Germany may be attributed to boundary effects of the model. In the target region of CECILIA the increase is strongest in a belt stretching from Austria over western Hungary and Serbia to Bulgaria.

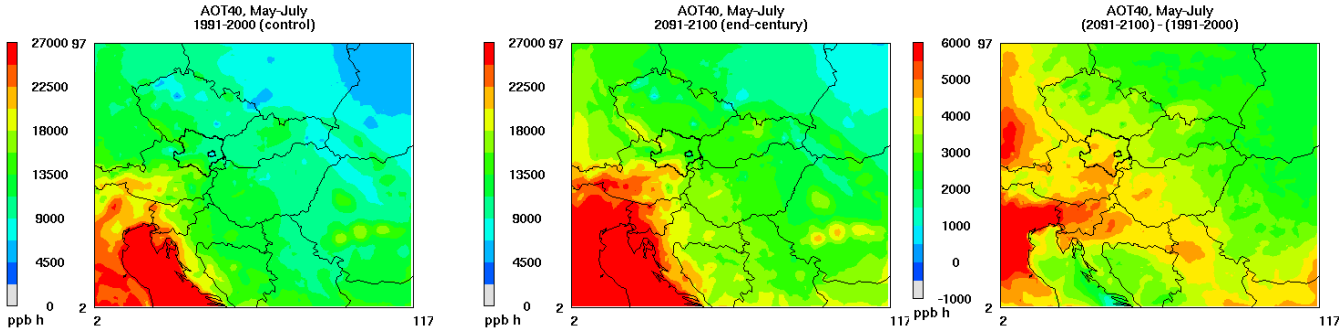

Figure 10. *Average of the $AOT40_c$ for May to July for the BOKU domain with 10 km spatial resolution for the present day decade 1991-2000 (left panel), for the end-century decade 2091-2100 (modele panel) and diference(right panel). Critical level for crops (EU), $AOT40_c$ = 9 000 ppb h.*

WUT

At WUT the RegCM3(Beta)-CAMx modelling system was implemented and validated for the WUT modelling domain, centred over Poland (52.00°N, 19.30°E) on a grid with 120 x 109 points and a resolution of 10 km. The original emission model EMIL (EMIssion modeL) was developed. The model applies for Poland and creates the so called second-level emission database for the high resolution 10 km photochemical runs performed at WUT. Emission database applied for other countries belonging to modelling domain remains zero-level (based on EMEP inventory). One of the main added value to the project was development of a detailed emission and stacks parameters database for a Large Combustion Plants (LCP) sources (with a stack height equal or above 100 m; $h \geq 100$ m) for PM_{10}, $PM_{2.5}$, SO_2, NO_x, NH_3 and NMVOC. Thus simulation of pollution plume from point sources was possible and constitutes the largest differences between air pollution modelling at WUT and at CUNI, AUTH and BOKU, where in CAMx simulations all sources were treated as surface area sources.

Results of the WUT modelling system runs for PM_{10}, $PM_{2.5}$ and SO_2 are presented in Figs. 11, 12 and 13, respectively. Left panels show calculated annual mean levels for the control period (1991-2000). The highest PM_{10} and $PM_{2.5}$ levels were obtained for the central and southern Poland. It should be pointed out, that in second-level detailed emission database prepared for Poland, emissions of PM and SO_2 were significantly higher than in zero-level database based on EMEP inventories. For SO_2 the highest concentrations were obtained for Silesia region in Poland as well as for Hungary and Ukraine. The high SO_2 concentrations calculated for Hungary and Ukraine are due to the treatment of LCP sources as surface area sources in zero-level emission database. Results of comparison between pollutant levels for control and for future periods given as differences in Figs. 11-13 (middle and right panels) show that climate change impacts on air pollution levels are small to moderate, and have different direction depending on pollutant concerned. For PM, decrease in concentrations (up to -3.5 $\mu g/m^3$) in future decades relative to control period in most of the countries is predicted. The exception of that trend is noted only for the Northern Germany, where slight increase in 2041-2050 period is observed. For SO_2 higher concentrations (up to 3.5 $\mu g/m^3$) are predicted in the future. The highest increase is expected for Upper Silesia region in Poland as well as for Northern Hungary.

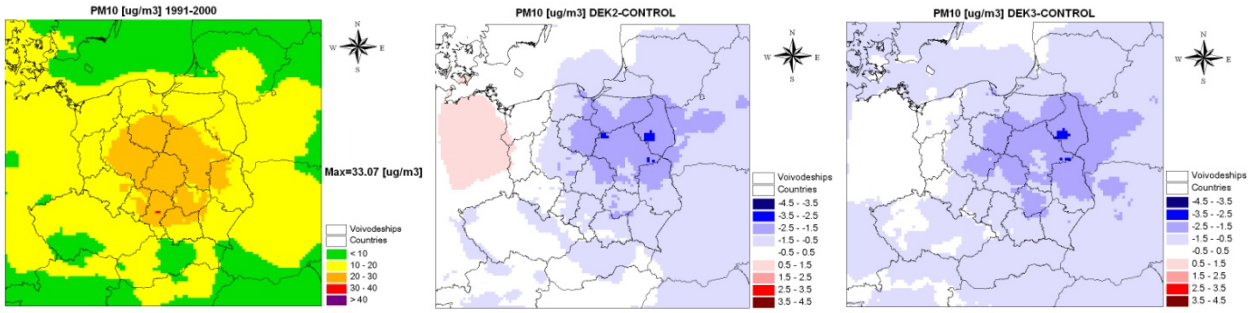

Figure 11. *Annual mean PM_{10} concentrations [$\mu g/m^3$] at WUT domain for control run 1991-2000 (left panel), and climate change impacts on PM_{10} concentrations in terms of the differences [$\mu g/m^3$] for 2041-2050 period (middle panel) and 2091-2100 period (right panel) against the control period 1991-2000.*

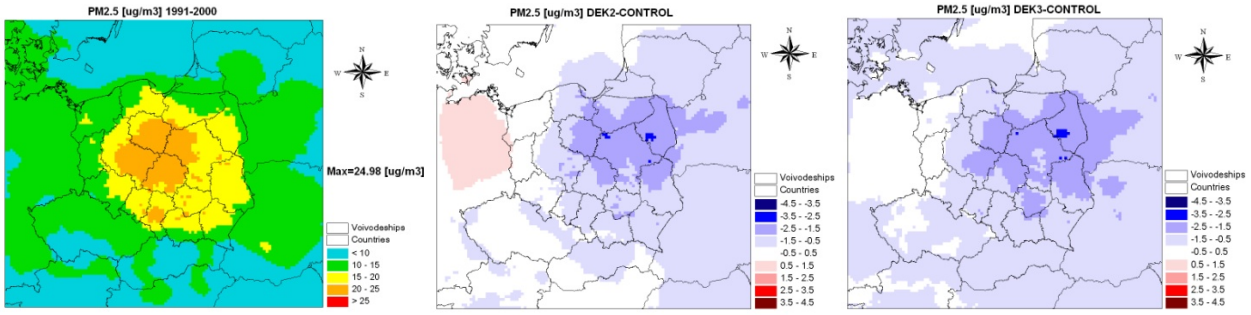

Figure 12. *Annual mean $PM_{2.5}$ concentrations [$\mu g/m^3$] at WUT domain for control run 1991-2000 (left panel), and climate change impacts on $PM_{2.5}$ concentrations in terms of the differences [$\mu g/m^3$] for 2041-2050 period (middle panel) and 2091-2100 period (right panel) against the control period 1991-2000.*

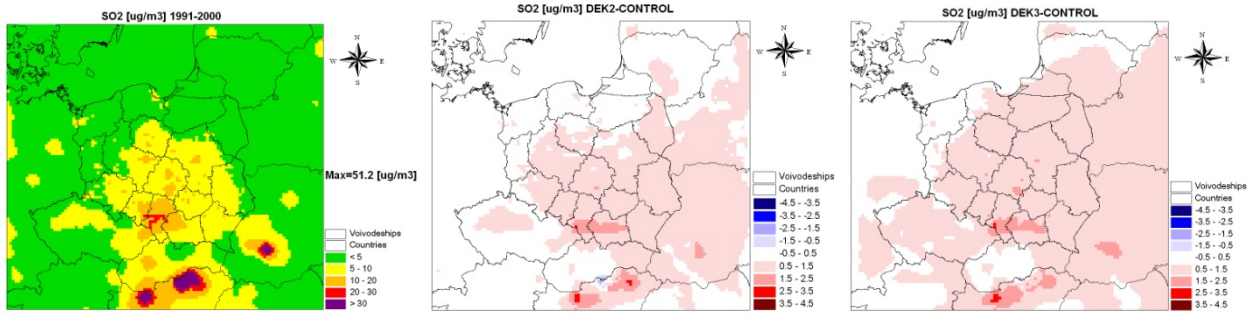

Figure 13. *Annual mean SO_2 concentrations [$\mu g/m^3$] at WUT domain for control run 1991-2000 (left panel), and climate change impacts on SO_2 concentrations in terms of the differences [$\mu g/m^3$] for 2041-2050 period (middle panel) and 2091-2100 period (right panel) against the control period 1991-2000.*

Left panels of Figs. 14, 15 and 16 show the distribution of total deposition calculated for the control period of oxidized sulphur, oxidized nitrogen and reduced nitrogen, respectively. The high deposition of sulphur were obtained for central-southern part of the domain, while for rest of the domain deposition is smaller. For oxidized nitrogen the deposition is smaller and its distribution is different. For the southern-western part of domain as well as for the Baltic coast line, bigger depositions were obtained. For reduced nitrogen the biggest depositions were calculated for Southern Germany, Belarus and Central Poland. Results of comparison between S and N deposition for control and for future periods given as differences in Figs. 115-117 (middle and right panels) show that climate change impacts on air pollutants deposition are small to moderate, and that climate change is causing increase in deposition of all acidifying species. The increase has growing trend from near to far future. The exception is sulphur deposition in the vicinity of large point sources in Poland, Ukraine and Hungary which is decreasing with descending trend in future climate. The increase of species deposition is most probably due to increase of precipitation (wet deposition) and wind speed (dry deposition) in future climate in the region under concern. The biggest increase of total deposition is predicted for the mountains areas within the domain: Bohemian Forest, Ore Mountains, Sudety Mountains and Carpathian Mountains.

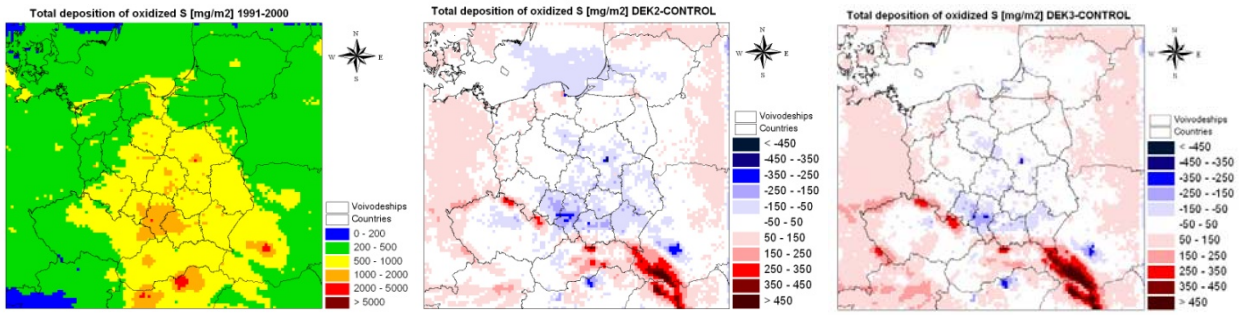

Figure 14. *Total deposition of oxidized sulphur [mg/m^2] for control run 1991-2000 (left panel), and climate change impacts on total deposition of oxidized sulphur in terms of the differences [mg/m^2] for 2041-2050 (middle panel) and 2091-2100 (right panel) against the control period 1991-2000.*

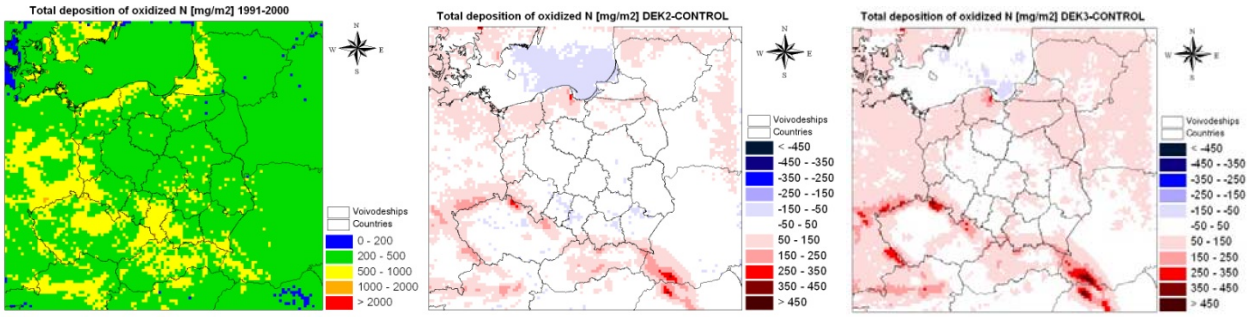

Figure 15.*Total deposition of oxidized nitrogen [mg/m^2] for control run 1991-2000 (left panel), and climate change impacts on total deposition of oxidized nitrogen in terms of the differences [mg/m^2] for 2041-2050 (middle panel) and 2091-2100 (right panel) against the control period 1991-2000.*

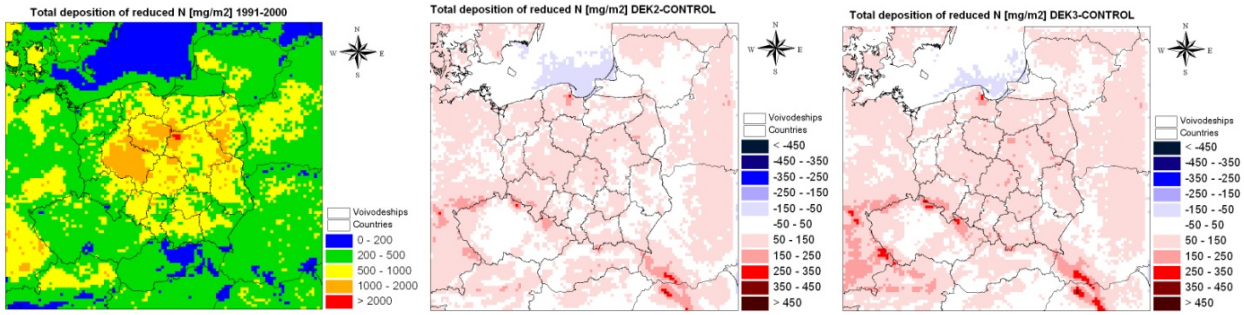

Figure 16. *Total deposition of reduced nitrogen [mg/m^2] for control run 1991-2000 (left panel), and climate change impacts on total deposition of reduced nitrogen in terms of the differences [mg/m^2] for 2041-2050 (middle panel) and 2091-2100 (right panel) against the control period 1991-2000.*

For the purpose of WP7 of CECILIA and Deliverable D7.4, *Guidelines for operational evaluation of the AQ-CTMs under WP7 of the CECILIA project* have been prepared by a group leader, Katarzyna Juda-Rezler (see D7.4 APPENDIX). The paper addresses Air Quality – Chemical Transport Models (AQ – CTMs) evaluation in terms of operational evaluation, which is aiming on comparing model results with measurements of species concentrations for a specific time period.

For final evaluation performance, a subset of parameters, which characterise the general uncertainties estimation, was applied. The subset consists of the following measures: NMB (Normalized Mean Bias), RMSE (Root Mean Square Error), with its systematic ($RMSE_s$) and unsystematic ($RMSE_u$) part, NMSE (Normalized Mean Square Error), correlation coefficient (r), IA (Index of Agreement) and FAC2 – a fraction of predictions within a factor 2 of observations. The formulas are given in D7.4 APPENDIX.

RegCM-EMIL-CAMx modelling system was evaluated for PM_{10} and SO_2 concentrations using observations from EMEP (http://www.emep.int) and EIONET-Airbase (http://air-climate.eionet.europa.eu) databases. For PM_{10} evaluation, data from IfT (Leibniz Institute for Tropospheric Research, Germany) research station Melpitz were also used. The Melpitz research station is one of the European station with the longest PM observations. For the reference year 2000, 30 stations for PM_{10} and 93 for SO_2 were available for model evaluation. Unfortunately, in Poland, there was only one such station for PM_{10} and 5 stations for SO_2. Both qualitative analysis (scatter plots, time series) and quantitative analysis were performed.

For evaluation of annual mean model predictions, the scatter plots of the predicted versus observed annual mean PM_{10} and SO_2 concentrations in 2000 together with calculated values of statistical indices are given in Fig. 118, whereas the values of statistical indices are given in the Tab. 1 as well. For annual means, evaluation results indicate a satisfactory model performance for both pollutants, however model performance for SO_2 is better than for PM_{10}. For PM_{10}, the observations are in general underestimated.

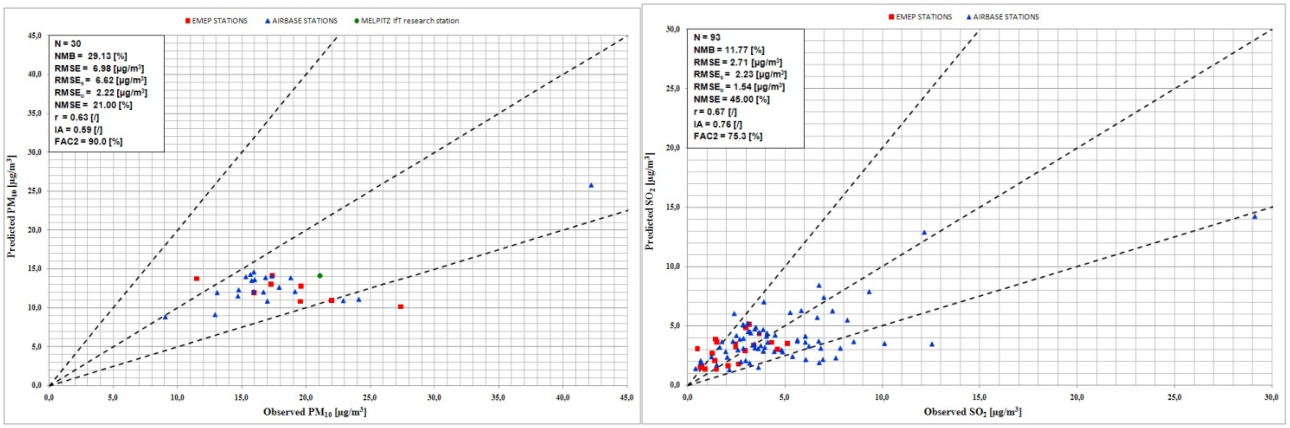

Figure 17. *The scatter plot of the predicted and observed annual mean PM_{10} levels (left panel) and annual mean SO_2 levels (right panel) for WUT domain (year 2000).*

Table 1. *Evaluation results of the RegCM–EMIL–CAMx modelling system for 2000 reference year.*

Statistical measures	PM_{10} annual mean	PM_{10} daily mean	SO_2 annual mean
N – number of samples	30	10 188	93
NMB – Normalised Mean Bias [%]	29.13	27.20	11.77
RMSE – Root Mean Square Error [µg/m^3]	6.98	12.92	2.71
$RMSE_s$ – Systematic Root Mean Square Error [µg/m^3]	6.62	10.85	2.23
$RMSE_u$ – Unsystematic Root Mean Square Error [µg/m^3]	2.22	7.02	1.54
NMSE – Normalised Mean Square Error [%]	21.00	73.20	45.00
r – Correlation coefficient [/]	0.63	0.33	0.67
IA – Index of Agreement [/]	0.59	0.55	0.76
Predictions within a factor of 2 of the observations [%]	90.00	64.00	75.30

The scatter plot of the predicted versus observed daily mean PM_{10} levels in 2000 is given in Fig. 18, while the statistical indices are given in Tab. 1 as well. Moreover the time series of daily mean PM_{10} values are presented for two stations: IfT research station in Melpitz, Germany and Kuznia, Poland (Fig. 120).

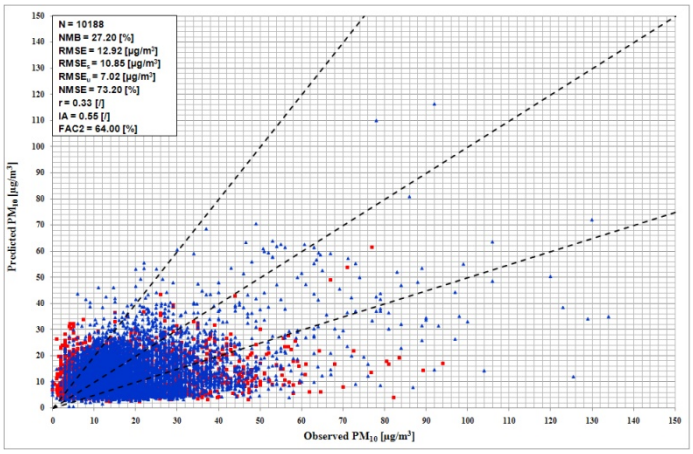

Figure 18. *The scatter plot of the predicted and observed daily mean PM_{10} levels for WUT domain (year 2000). Dashed lines indicate perfect agreement (middle line) and a difference of a factor of 2.*

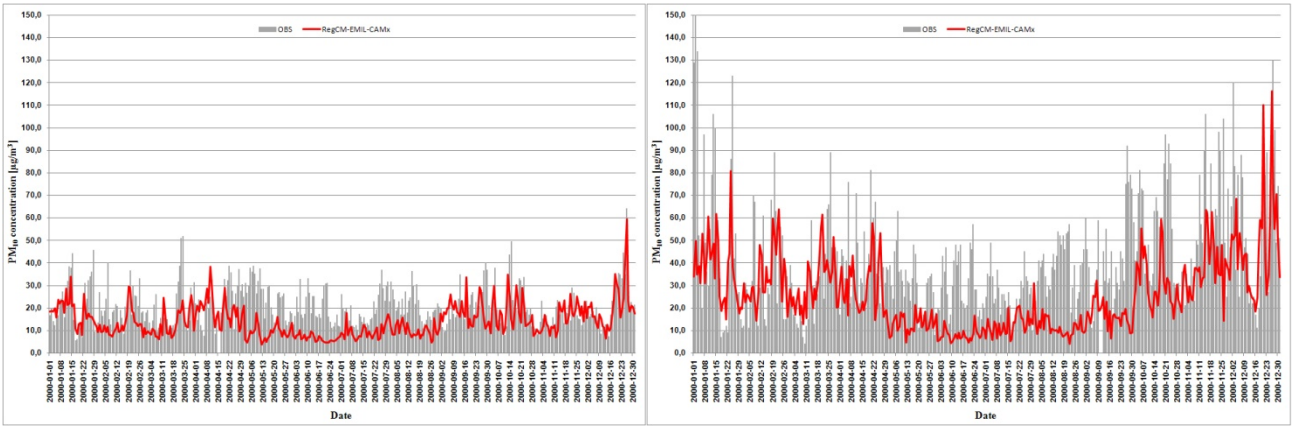

Figure 19. *Observed and calculated PM_{10} time series of daily mean concentrations at Melpitz IfT research station, Germany (left panel) and at Kuznia, Poland (right panel) – year 2000. Observed data from Melpitz by courtesy of dr Gerald Spindler (IfT, Leipzig, Germany).*

As it can be seen in Tab. 1 for daily mean predictions, evaluation results indicate poorer model performance than for annual means. This is quite understandable taking into account the specific of PM_{10} air pollution, which is due to both natural and anthropogenic sources, moreover it is both primary and secondary pollutant. Still, when comparing predicted and observed time-series it can be noted that during winter, the patterns of measured PM_{10} levels are fairly well simulated by the RegCM-EMIL-CAMx modelling system. For Melpitz research station winter PM_{10} levels, specially for January and October-December, are well predicted by model and peak values are well captured. During summer the model performance is worse. For Polish station Kuznia, model performance is better in winter than in summer as well. Overall, the predicted pattern of measured time series in Kuznia is poorer than in Melpitz, however model is also able to capture peak, up to 115 $\mu g/m^3$, values.

Summarizing, the ability of the modelling system to simulate PM_{10} and SO_2 concentrations in Central-Eastern Europe is promising. Detailed emission data provided by the emission model EMIL play important role in improving the model performance.

NIMH

The climatic version of the operational weather forecast model ALADIN was applied for simulating 3 time slices: 1960-2000 (Control Run, CR), 2020-2050 (Near Future, NF) and 2070-2100 (Far Future, FF), following the IPCC scenario A1B (CECILIA WP1 and WP2). The calculations are made for an area covering Bulgaria region with resolution of 10 km. The created meteorological database is used to estimate the impact of climate changes on air quality.

A modeling system was created on the base of US EPA Models-3 tool (MM5, CMAQ and SMOKE) and a number of interface FORTRAN programs and Linux scripts capable to long-term simulation for a nested region with resolution of 10 km covering Bulgaria. TNO emission inventory for 2000 is used for all time slices. The chemical boundary conditions (BC) are extracted from a database containing results of 50-km RegCM3/CAMx runs over Europe made by AUTH. CMAQ boundary points values are calculated off-line in AUTH, results downloaded to a server in NIMH. There, the BC input files are being prepared in-line by another interface program during the simulations. For year 2000, some scenarios are run, results compared with measuring data. The comparisons point out the good simulation quality of the System.

There are quite few measurements in the territory of Bulgaria capable to be used for comparison with calculations. There is no EMEP station in the ALADIN/CMAQ domain. The automated and sampling stations, operated by Bulgarian EPA are placed in the most polluted areas – big cities and industrial regions and cannot be used for comparison with the model results that more or less describe background conditions. Only one official background station exists in the country – the peak Rojen, Rhodopi mountain (41N41, 24E44, altitude 1700 m), but there is no regular ozone and PM measurements available in the investigated period. Fortunately, during all the year 2000 in the frame of research project (Donev et al., 2002; Georgiev and Donev, 2006) hourly ozone measurements have been performed at peak Rojen and Ahtopol, small town at Black sea cost (42N05, 27E57, altitude 10 m). This data were the main source for validating the model results. Another set of measurements is dust probes sampling on daily basis in NIMH, Sofia (49N39, 23E23, altitude 550 m). The station is placed on the south-east vicinity of the town at a highways crossroad. No special measures were taken to distinguish particles by size. Nevertheless, this data is also used for comparison with PM_{10} model results. The measurement points are shown in Fig. 20.

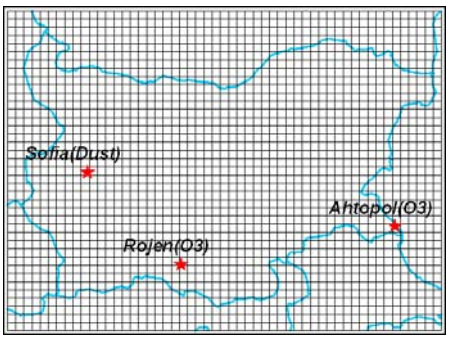

	Anthropogenic sources		Natural sources	Both types
Scenario	AS	LPS	BgS	BC
A (basic)	Y	Y	Y	Y
B	Y	Y	Y	
C	Y	Y		Y
D	Y	Y		

Figure 20. *Measurement points in NIMH domain (left) and scenarios description (right).*

For year 2000 four scenarios, presented in Fig. 125, were calculated. The aim is to estimate the importance of biogenic emissions and the boundary conditions. The lack of boundary conditions means zero-values of all variables in all boundary points.

In Fig. 21 the yearly variation of the row data and three model scenarios are displayed. It is clearly seen that Scenario A demonstrates more or less good agreement with measurements. The biggest discrepancy is in Rojen for the first 3 months of the year. In that period problems with measurement equipment happened; there is a big gap in data (February – March). Scenarios B and D demonstrate quite low ozone levels (less than one third of the basic case) that reflects the extremely high importance of the use of reliable boundary conditions for obtaining realistic model results. The smaller the region of calculation is the more important BC are.

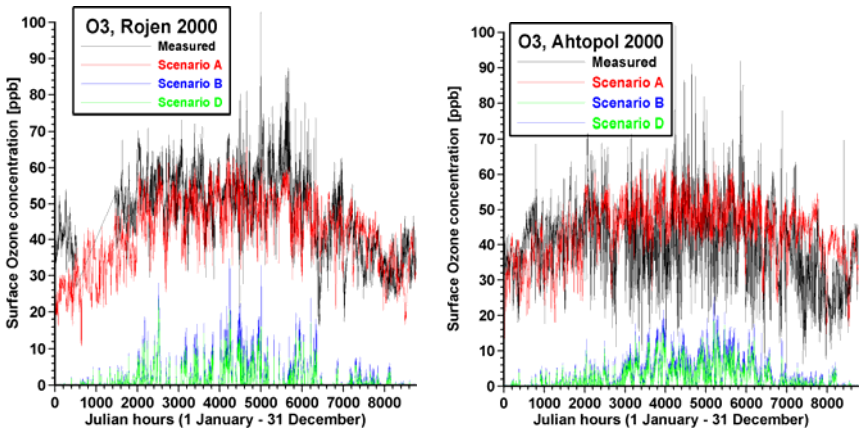

Figure 21. *Yearly variation of measured and calculated ozone (1-hour data).*

As it can be noticed in Fig. 22, the results of Scenario C (Basic Scenario with Biogenic emissions switched off) are much close to those of Scenario A (two left graphs). The exclusion of biogenic emissions slightly decreases the ozone values. All this shows that in the Basic case the fluxes through the boundaries are dominating in ozone formation leading to the so called "VOC-saturated" regime.

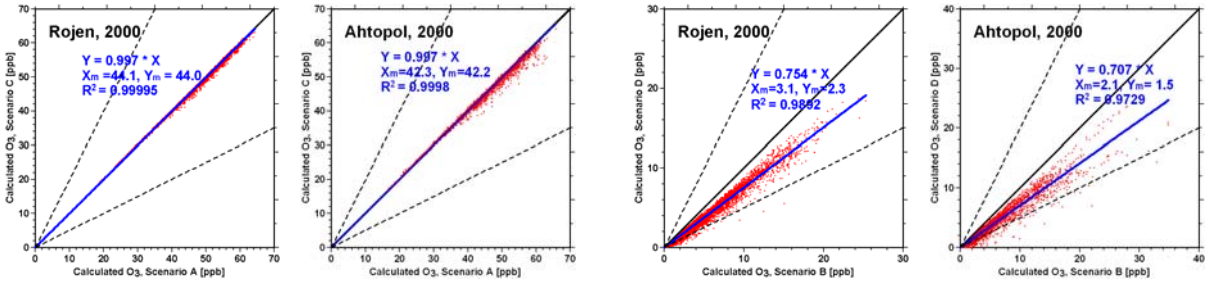

Figure 22. *Scenarios comparison: A vs. C (left two graphs) and B vs. D (right two graphs)*

In contrary, the right two graphs in Fig. 22 (cases with zero fluxes through the boundaries, Scenarios B and D) show that the biogenic emissions are very important – the ozone values become 20-30% lower when this emission source is switched off.

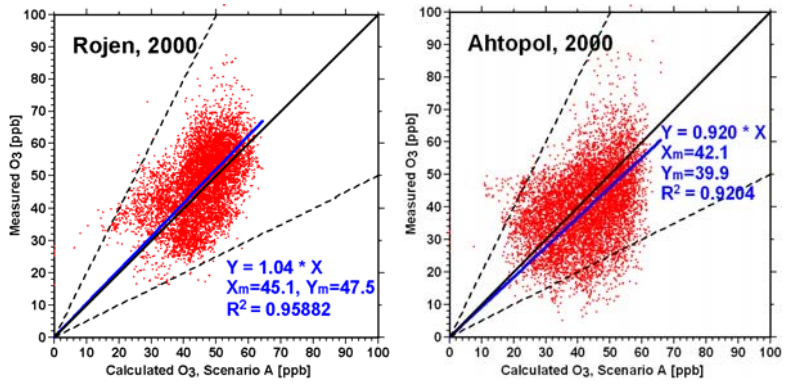

Figure 23. *Scatter diagrams of measurement and modeled (Scenario A) 1-hour data.*

The scatter diagrams of Scenario A *vs.* measurements are displayed in Fig. 23. Almost all scatter points are into FAC2 boundaries (dashed lines). The fitting lines are quite close to the ideal fitting line showing slight underestimation of measurement data in Rojen and somewhat bigger (but still small) overestimation in Ahtopol. The correlation coefficients of both fits are quite high that reflects the good quality of the simulation.

High ozone concentrations can cause damages on plants, animals and human health. In fact, when the effects from high ozone levels are studied, one should look not at the ozone concentrations but on some related quantities. The following four quantities were calculated (see e.g. Zlatev and Syrakov, 2004):

- **$AOT40_c$ values,** which are damaging crops when they exceed 3000 ppb.hours.
- **$AOT40_f$ values,** which are damaging forests when they exceed 10000 ppb.hours.
- **NOD60 (**Number Of Days in which the day-time 8 hours running averages over ozone concentration exceed the critical value of 60 ppb). If the limit of 60 ppb is exceeded at least once during a given day the day is considered "bad". People with asthmatic diseases have difficulties in "bad" days. The requirement is often relaxed to maximum 25 "bad" days in the period April-September.
- **ADM** (Averaged Daily Maxima) of the ozone concentrations in the period from April 1 to September 30. This quantity is not directly related to some particular damaging effects. However, it is convenient to validate the model results when this quantity is used.

Table 2. *Ozone indexes calculated from measurement and simulation (Scenario A) data*

Stations	**Index**	**$AOT40_c$**	**$AOT40_f$**	**NOD60**	**ADM**
	Period (2000)	MJJ	AMJJAS	AMJJAS	AMJJAS
Rojen	Measured	20300	29300	27	59.3
	Calc.(Sc. A)	18500	26800	7	54.4
Ahtopol	Measured	8020	12700	12	54.1
	Calc.(Sc. A)	17100	24100	7	53.6

In Tab. 2, the calculated ozone indices for both measurement stations are presented. The calculated and measured ADMs are quite close for both stations while quite big differences in the other ozone indices can be noticed. The reason is the sensitivity of these indices to the model and measurement errors, discussed in detail in Zlatev and Syrakov (2004). In any case, it is seen that both calculated and measured indices overcome 1.5-2 times the respective thresholds. The calculated AOT40 values are closer to the measured ones for Rojen than for Ahtopol. The calculated NOD60 are rather different from the measured ones. Both of them are about and under the threshold of 25 days.

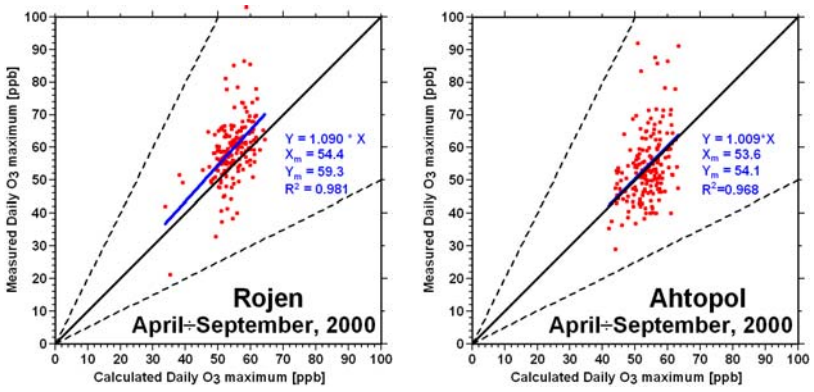

Figure 24. *Scatter diagrams of measured vs. calculated Daily Maxima.*

As far as the best way to compare ozone data is the usage of daily maxima, in Fig. 24 the scatter diagrams of measured *vs.* calculated daily maxima for both stations are displayed. One can notice that the fitting lines are very close to the ideal line, correlation coefficients being over 0.95. This figure also support the conclusion made interpreting Fig. 23. The simulation results are rather good and can be used with certainty investigating the climate change impact on pollution levels. All statistics required in the frame of CECILIA WP7 (Juda-Rezler, 2009) are presented in Tab. 3.

Table 3. *Statistical criteria for validation of ALADIN/CMAQ ozone results (year 2000)*

Station Name	Ahtopol		Rojen	
	observation	m. prediction	observation	m. prediction
Location	coastal		mountain	
Latitude, dec.	42.12		41.88	
Longitude, dec.	27.95		24.73	
Altitude, m.	29		1750	
Measured pollutant	ozone		ozone	
Measurement frequency	1 hour		1hour	
Number of valid measurements/m.predictions	8614	8760	7776	8760
Data completeness, %	98.3	100	88.8	100
Summer (JJA) mean, microgram/m^3	87.37	99.57	107.38	98.92
Maximal 8-hour mean, microgram/m^3	90.74	87.34	101.68	93.72
93.15th perc. (from 8-h. daily max.), microgram/m^3	123.42	112.62	133.36	114.58
AOT40 (for veg. protection), ppb.h	9392.97	14956.24	14127.92	14401.65
MB (from 8-h. daily max.), microgram/m^3	3.40		7.97	
NMB (from 8-h. daily max.), %	3.75		7.84	
NMSE (from 8-h. daily max.), %	5.68		4.15	
RMSE (from 8-h. daily max.), microgram/m^3	21.22		19.88	
RMSEs (from 8-h. daily max.), microgram/m^3	13.15		15.19	
RMSEu (from 8-h. daily max.), microgram/m^3	16.64		12.81	
r (from 8-h. daily max.)	0.52		0.61	
IA (from 8-h. daily max.)	0.70		0.71	
EXV (from 8-h. daily max.), %	13.00		23.27	
FAC2 (from 8-h. daily max.),%	97.96		99.69	
RPtvE (from 8-h. daily max.)	0.09		0.14	

Analogous conclusion, but not with the same certainty, can be derived from the comparison of calculated PM_{10} concentration in NIMH, Sofia, and the measured daily Total Dust Content (TDC). The main difficulty is that there are not direct measurements of PM_{10} and its estimation from TDC is quite uncertain. In the literature, various ratios PM_{10}/TDC are described (mainly from 0.2 to 0.7) depending on many different factors including the source categories and weather conditions. As to make at least qualitative conclusion about CMAQ simulation quality, two cases are displayed in Fig. 25. In the first one, calculated PM_{10} is compared with 0.15*TDC. In the second graph, TDC is replaced with a sample containing only the measurements with dust concentrations less than 60 $\mu g/m^3$. The reason of this modification is that the big measured values are probably obtained in windy days when big (and heavy) particles can get on the filter. It is supposed that in such a way obtained sample the particles are suspended in the air and it is called Total Suspended Particulate (TSP) which differs from TDC. It can be seen from both scatter diagrams that CMAQ calculations simulate in a satisfactory way the reasonable estimates of measured PM_{10} (the ratio PM_{10}/TDC at the lower limit of its reference values). All this confirms again that the ALADIN/CMAQ system is able to give reliable assessment of climate change impact on air quality.

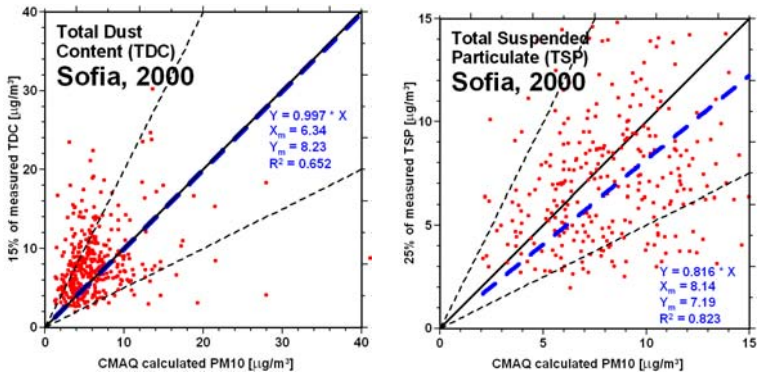

Figure 25. *Comparison of calculated PM_{10} and the measured dust (estimated PM_{10}). Right graph contains measured dust concentrations less than 60 $\mu g/m^3$, only.*

The evaluation of ALADIN/CMAQ simulations showed that the modelling system has a satisfactory performance with respect to O_3. Despite the using boundary conditions from another modelling system (RegCM3/CAMx with resolution 50 km) the basic spatial and temporal O_3 patterns are captured by the model. The best simulation quality refers summer time daily maximums. There are essential discrepancies when estimating the O_3 indexes recommended by EU Ozone Directive. The reasonable performance of the ALADIN/CMAQ system for the present time simulations justifies its use for future time projections. The PM comparisons also support qualitatively this conclusion.

Following the technology just described, the 10-year period (1991-2000) of the CECILIA Control Run (CR) was simulated. The results of this simulation can be used both for estimating "climatic" pollution levels typical for the now-a-day period and for investigation of inter-annual variations of the air quality. In the left panel of Fig. 26, the "now-a-day climatic" ozone field is presented compared with the field of 10-year mean ADM. One can notice some resemblance between space patterns but the values are quite different – the maximum of climatic ozone field is of order of the minimum of ADM-field.

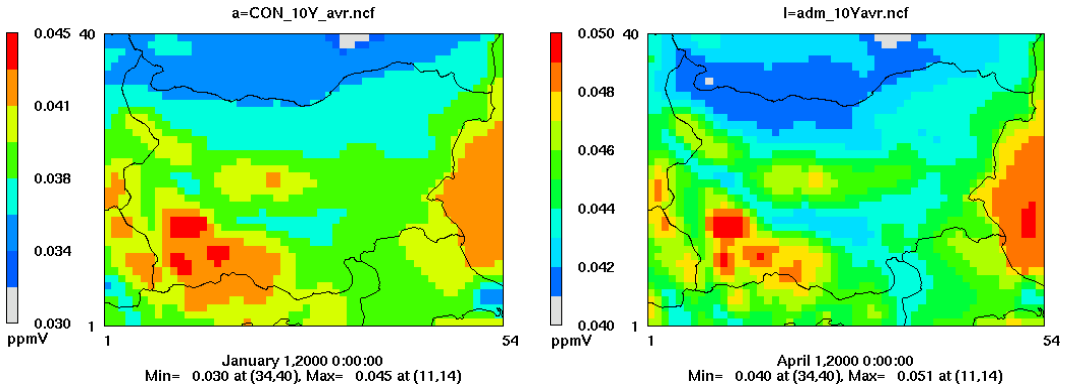

Figure 26. *10-year mean ozone concentration (left) and ADM (right), Control Run.*

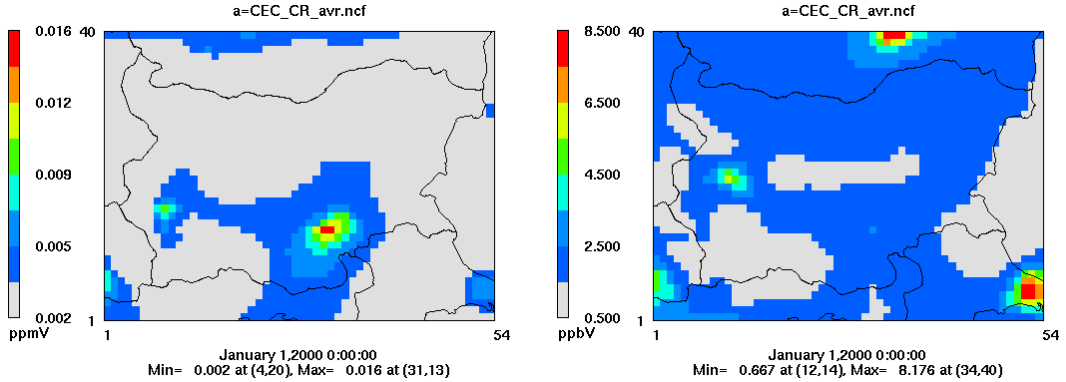

Figure 27. *10-year averaged fields of SO_2 (left) and NO_2 (right), Control Run.*

The SO_2-pollution (Fig. 27) has a well expressed maximum around the main source in the area - the three neighboring lignite coal burning thermal power plants (TPP Mariza-Iztok) in southeast Bulgaria and secondary maximum in west Bulgaria, around the TPP Bobov dol. In the NO_2-field the most populated areas form the respective maximums. They are in the region of Sofia (inside the country) but most of all they are expressed outside Bulgaria – towns of Bucharest (Romania, up) and Istanbul (Turkey, down-right). In the remaining part of Bulgaria, the NO_2 pollution levels are more or less evenly distributed. The minimums are well connected with the mountain areas (Balkan mountain in the middle, Rila-Rodipi mountains down-left and Sacar mountain down-right) as well as with Black sea area.

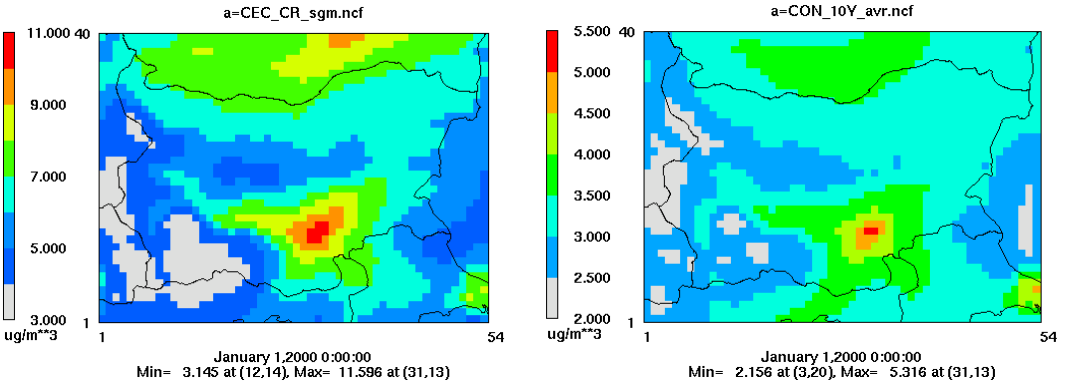

Figure 28. *10-year averaged fields of PM_{10} (left) and particulate sulphate (right), Control Run.*

In Fig. 28 the "climatic" fields of PM_{10} and PSO4 are displayed. The both fields are most or less similar that can be expected. Their main maximums are again around the most powerful PM source – TPP Maritza-Iztok in the centre. The two other spots are due to Istanbul (Turkey) and Bucharest (Romania). No other peculiarities in PM distribution can be noticed.

Similarly, the simulations for the near (2041-2050) and far (2091-2100) future decades were performed. The space distribution of the interpreted above 4 main pollutants (SO_2, NO_2, PM_{10} and Ozone ADM) are presented in Figs. 29 and 30 for near and far future periods, respectively.

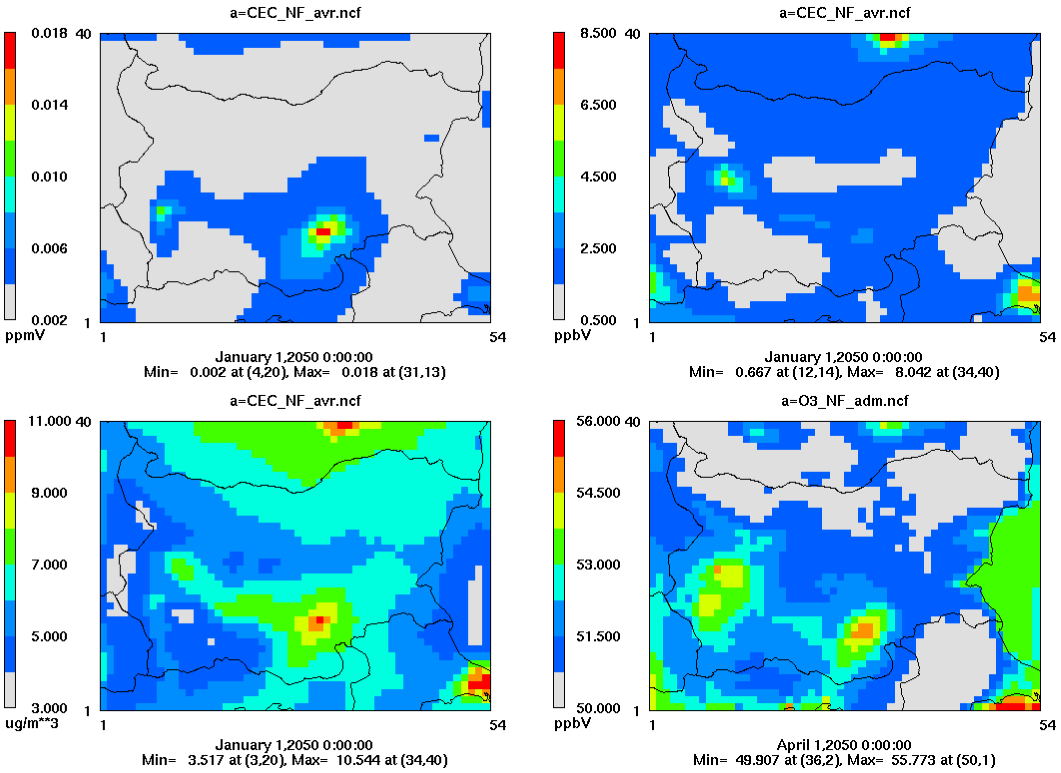

Figure 29. *10-year averaged fields of SO_2 (upper left), NO_2 (upper right), PM_{10} (bottom left) and ozone ADM (bottom right) for Near Future (2041-2050).*

It is clearly seen that the main pollution sources are well expressed again. More or less, all fields show almost the same special distribution as the respective pollutants from the Control Run.

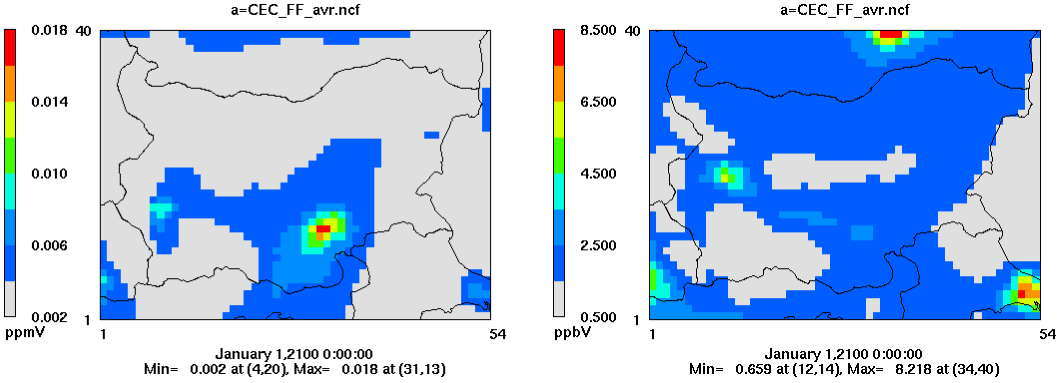

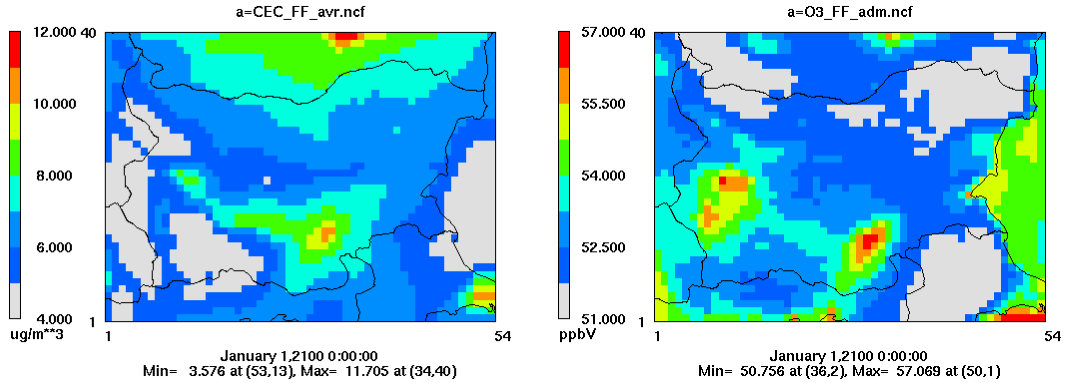

Figure 30. *10-year averaged fields of SO_2 (upper left), NO_2 (upper right), PM_{10} (bottom left) and ozone ADM (bottom right), Far Future (2091-2100).*

In Figs. 31, 32 and 33 the special distribution of the differences in 10-year mean concentrations for the 3 time slices are presented for SO_2, NO_2, and O_3, respectively. It can be clearly seen, that the differences are not very big as a whole. For all 3 species the differences between near future (NF) and control run (CR) as well as between far future (FF) and CR are bigger that those between FF and NF.

For SO_2 (Fig. 31) the maximum differences are about 2 ppb that is of order of 10 % from the maximal values. These maximums are distributed mainly in the region of the main pollution source (TPP Mariza-Iztok) or in their plumes. The highest values of this differences are observed in the Far Future against the Control Run. The differences between the Far and Near future are rather small (please notice the different scale).

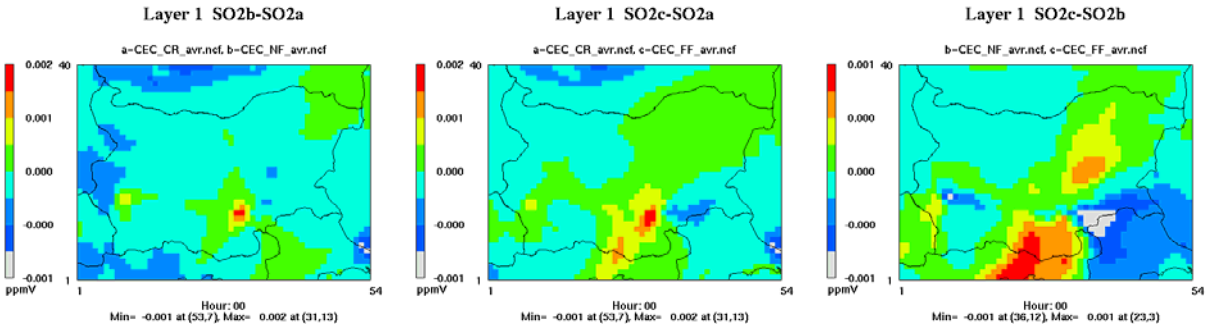

Figure 31. *Differences in the 10-year SO_2 mean fields for "NF-CR" (left), "FF-CR" (middle) and "(FF-NF) (right).*

The mean NO_2 concentration is arising from period to period almost in the whole domain (Fig. 137). Only in the regions of Istanbul and Bucharest negative values can be noticed. The differences "FF-CR" show again biggest values and spatial distribution. In prevailing part of the domain, NO_2 concentrations differences are close to zero. The highest differences are relatively small in comparison with concentration maxima – about 5 % that is below the uncertainty level.

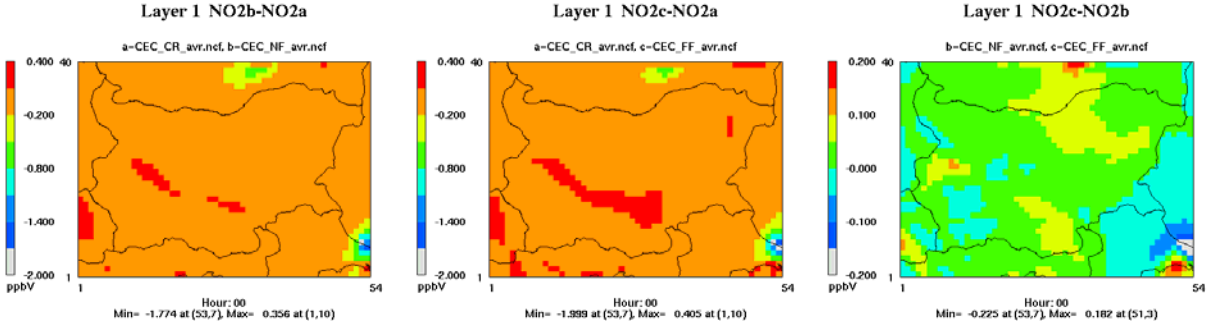

Figure 32. *Differences in the 10-year NO_2 mean fields for "NF-CR" (left), "FF-CR" (middle) and "(FF-NF) (right).*

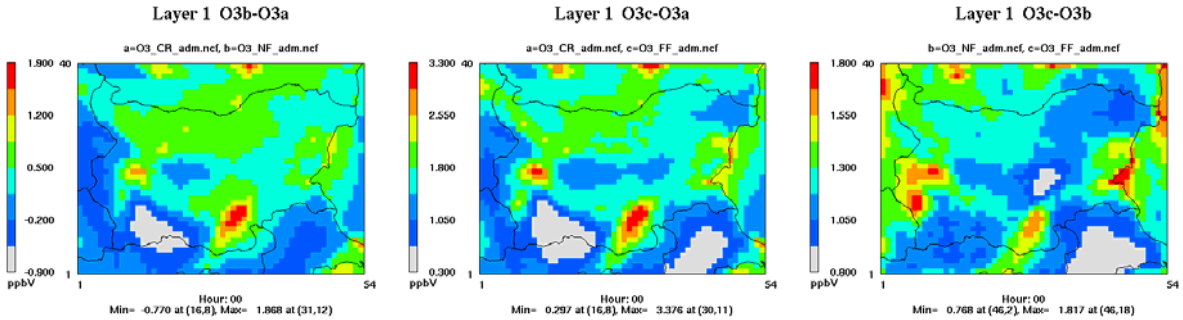

Figure 33. *Differences in the 10-year ozon ADM fields for "NF-CR" (left), "FF-CR" (middle) and "(FF-NF) (right).*

For Ozone ADM (Fig. 33) the biggest differences are between FF and CR. The highest values are over 3 ppb, that is again about 5 % of ADM maxima, i.e. not significant. There is a definite separation between positive and negative difference values in both cases (NF-CR) and (FF-CR) – they are positive in the plain parts of the domain and negative in the mountain areas. The mean ADM concentration is arising from period to period almost in the whole domain. Again the plumes of the main pollution sources show maximal values, but that time a new source appear at the Black Sea cost – the Lokoil refinery near the town of Burgas.

References

Cohen A.J., Anderson H.R., Ostro B., Pandey K.D., Krzyzanowski M., Kunzli N., Gutschmidt K., Pope A., Romieu I., Samet J.M., Smith K., 2005. The global burden of disease due to outdoor air pollution. Journal of Toxicology and Environmental Health - Part A - Current Issues, 68, 1301-7.

Donev E., Zeller K., Avramov A., 2002. Preliminary background ozone concentrations in the mountain and coastal areas of Bulgaria. Environmental Pollution, 17, 281-286. Elguindi, N., X. Bi, F. Giorgi, B. Nagarajan, J. Pal, F. Solmon, S. Rauscher, A. Zakey, 2006: RegCM Version 3.1 User's Guide. PWCG Abdus Salam ICTP.

EC, 2008. Directive 2008/50/EC of the European Parliament and of the Council of 21 May 2008 on ambient air quality and cleaner air for Europe.

Elguindi N., Bi X., Giorgi F., Nagarajan B., Pal J., Solmon F., Rauscher S., Zakey A., 2006. RegCM Version 3.1 User's Guide. PWCG Abdus Salam ICTP.

ENVIRON Corp., 2006: CAMx Users' Guide, version 4.40

EPA, 1999. The Benefits and Costs of the Clean Air Act 1990 to 2010: EPA Report to Congress. U.S. Environmental Protection Agency, Washington D.C.

Georgiev K., Donev E., 2006. On some ozone studies: comparison of model results and measurements over the territory of Bulgaria. Problems in Programming, 8, No. 2-3, 767-770.

Gery, M.W., G.Z. Whitten, J.P. Killus, and M.C. Dodge. 1989: A Photochemical Kinetics Mechanism for Urban and Regional Scale Computer Modeling. J. Geophys. Res., 94, 925-956.

Giorgi, F., X. Bi, Y. Qian, 2002: Direct radiative forcing and regional climatic effects of anthropogenic aerosols over East Asia: A regional coupled climate-chemistry/aerosol model study. .J. Geophys. Res., 107, 4439, doi:10.1029/2001JD001066.

Giorgi, F., Y. Huang, K. Nishizawa and C. Fu, 1999: A seasonal cycle simulation over eastern Asia and its sensitivity to radiative transfer and surface processes. Journal of Geophysical Research, 104, 6403-6423.

Guenther, A.B., Zimmerman, P.R., Harley, P.C., Monson, R.K., and Fall, R., 1993: Isoprene and monoterpene rate variability: model evaluations and sensitivity analyses, J. Geophys. Res., 98, No. D7, 12609-12617.

Guenther, A. , Zimmerman, P., and Wildermuth, M., 1994: Natural volatile organic compound emission rate estimates for U.S. woodland landscapes, Atmospheric Environment, 28, 1197-1210.

Juda-Rezler K., 2004. Risk Assessment of Airborne Sulphur Species in Poland. In: Air Pollution Modelling and its Application XVI, eds.: C. Borrego & S. Incecik, Kluwer Academic/Plenum Publishers, New York 2004, 19-27.

Juda-Rezler K., 2009. Guidelines for operational evaluation of the AQ-CTMs under WP7 of the CECILIA project, version 1.1, July, 16th, 2009. Manuscript.

Katragkou, E., P. Zanis, I. Tegoulias, D. Melas, 2009: Tropospheric ozone in regional climate-air quality simulations over Europe: Future climate and sensitivity analysis. Proceedings 30th NATO/SPS International Technical Meeting on Air Pollution Modelling and its Application.

Katragkou E., Zanis P., Tegoulias I., Melas D., Krüger B.C., Huszar P., Halenka T., Rauscher S., 2009. Decadal regional air quality simulations over Europe in present climate: near surface ozone sensitivity to external meteorological forcing. Atmos. Chem. Phys. Discuss., 9, 10675-10710.

Katragkou E., Zanis P., Tegoulias I., Kioutsioukis I., Melas D., 2010. Surface ozone in regional climate-air quality simulations over Europe: Future climate and sensitivity analysis. Submitted to JGR.

Krüger B. C., E. Katragkou, I. Tegoulias, P. Zanis, D. Melas, E. Coppola, S. Rauscher, P. Huszar and T. Halenka, 2008: Regional decadal photochemical model calculations for Europe concerning ozone levels in a changing climate, Quarterly J. of the Hungarian Meteorol. Service, Idojaras, 112, 3–4, 285–300.

Makra L., Brimblecombe P., 2004. Selections from the history of environmental pollution, with special attention to air pollution. Part 1. International Journal of Environment and Pollution, 22, 641-56.

Pal, J. S., F. Giorgi, X. Bi, N. Elguindi, F. Solmon, X. Gao, S. A. Rauscher, R. Francisco, A. Zakey, J. Winter, M. Ashfaq, F. S. Syed, J. L. Bell, N. S. Diffenbaugh, J. Karmacharya, A. Konaré, D. Martinez, R. P. da Rocha, L. C. Sloan, and A. L. Steiner, 2007: Regional Climate Modeling for the Developing World: The ICTP RegCM3 and RegCNET. Bull. Amer. Meteorol. Soc., 88, 9, 1395–1409.

Pope C.A., Burnett R.T., Thun M.J., Calle E.E., Krewski D., Ito K., Thurston G.D., 2002. Lung cancer, cardiopulmonary mortality, and long-term exposure to fine particulate air pollution. Journal of the American Medical Association, 287, 1132–1141.

Pope C.A., Dockery D.W., 2006. Health effects of fine particulate air pollution: Lines that connect. Journal of the Air & Waste Management Association, 56, 709-42.

Qian, Y., F. Giorgi, 2000: Regional climatic effects of anthropogenic aerosols? The case of Southwestern China, Geophys. Res. Lett., 27(21), 3521-3524, 10.1029/2000GL011942.

Qian, Y., F. Giorgi, Y. Huang, W.L. Chameides, and C. Luo, 2001: Simulation of anthropogenic sulfur over East Asia with a regional coupled chemistry/climate model. Tellus, Ser. B, 53, 171-191.

Simpson, D., Fagerli, H., Jonson, J., Tsyro, S., and Wind, P., 2003. Transboundary Acidification, Eutrophication and Ground Level Ozone in Europe PART I, Norwegian Meteorological Institute.

Tuomisto J.T., Wilson A., Evans J.S., Tainio M. (2008). Uncertainty in mortality response to airborne fine particulate matter: Combining European air pollution experts. Reliability Engineering and *System Safety*, **93**, 732–744.

Visschedijk A.J.H., Denier van der Gon H.A.C., 2005. Gridded European anthropogenic emission data for NOx, SOx, NMVOC, NH3, CO, PPM10, PPM2.5 and CH4 for the year 2000. TNO-Report B&O-A R 2005/106.

Winiwarter W., Zueger, J., 1996. Pannonisches Ozonprojekt, Teilprojekt Emissionen. Endbericht. Report OEFZS-A-3817, Austrian Research Center, Seibersdorf.

Watkiss P., Pye S., Holland M., 2005. Baseline Scenarios for Service Contract for carrying out cost-benefit analysis of air quality related issues, in particular in the clean air for Europe (CAFE) programme. AEAT/ED51014/ Baseline Issue 5. Didcot, United Kingdom.

WHO, 2000. Air Quality Guidelines for Europe, 2nd edition. World Health Organization, Regional Office for Europe, Copenhagen.

WHO, 2005. Air Quality Guidelines. Global update 2005. World Health Organization, Regional Office for Europe, Copenhagen.

Zlatev Z., Syrakov D., 2004. A fine resolution modelling study of pollution levels in Bulgaria. Part 2: High ozone levels. *International Journal of Environment and Pollution*, **22**, No. 1-2, 203-222.